Submitted to

International Europhysics Conference on High Energy Physics, July 12, 2001, Budapest
EPS 2001: Abstract: **802**
Parallel Session **5,6**
XX International Symposium on Lepton and Photon Interactions, July 23, 2001, Rome
LP 2001: Abstract: **495**
Parallel Session **11**

www-h1.desy.de/h1/www/publications/conf/conf_list.html

Observation of isolated leptons with missing P_T and comparison to W production at HERA

H1 Collaboration

Abstract

A search for events with a high energy isolated lepton and missing transverse momentum has been performed at the electron-proton collider HERA using an integrated luminosity of 13.6 pb^{-1} in e^-p scattering and 101.6 pb^{-1} in e^+p scattering. Within the Standard Model such events are expected to be due to W boson production, with subsequent leptonic decay. The analysis has been tuned to maximise the acceptance of such events, and reject other Standard Model processes. In e^-p interactions no events are observed, consistent with the expectation of the Standard Model in this low luminosity sample. In the e^+p data 18 events are seen in the electron and muon channel compared to an expectation of 10.5 ± 2.5 dominated by W production (8.2 ± 2.5). The excess above the expectation is mainly due to events with transverse momentum of the hadronic system greater than 25 GeV where 10 events are found compared to 2.8 ± 0.7 expected.

1 Introduction

The HERA collaborations have previously reported [1, 2, 3] the observation of events with high P_T isolated leptons and missing transverse momentum in e^+p collisions during the period 1994-1997. The only Standard Model process which contributes significantly to this event signature is leptonic W decay. H1 has reported [2] one e^- event and 5 $\mu^\pm$ events compared to expectations from the Standard Model of 2.4$\pm$0.5 and 0.8$\pm$0.2 for the $e^\pm$ and $\mu^\pm$ channels respectively, which are dominated by W production. For the same data taking period ZEUS has reported [3] 3 (0) e^+ ($\mu^\pm$) events compared to an expectation of 2.1 (0.8) W events and 1.1 ± 0.3 (0.7 ± 0.2) background events for the $e^\pm$ ($\mu^\pm$) channel.

An extended analysis, developed to preferentially select events containing a high energy isolated electron or muon and missing transverse momentum, whilst rejecting other background processes, has also been presented in [4, 5]. In this paper we present the results of a similar search using the 36.5 pb^{-1} of e^+p data taken in 1994-1997 at an electron-proton cms energy of $\sqrt{s} = 300$ GeV , the 13.6 pb^{-1} of e^-p data (1998-1999, $\sqrt{s} = 318$ GeV) and the complete 65.1 pb^{-1} of e^+p data (1999-2000, $\sqrt{s} = 318$ GeV). ZEUS have also updated their analysis in [6].

This paper is organised as follows. Section 2 describes the Standard Model processes that contribute to the signal and to the background. Section 3 describes the H1 detector and experimental conditions. Section 4 outlines the lepton identification criteria and the hadronic reconstruction methods. The selection requirements and the results for the electron[1] and muon channels are described in sections 5 and 6. Section 7 discusses the kinematics of the selected events. The paper is summarised in section 8.

2 Standard Model Processes

In this section the processes within the Standard Model that are expected to contribute to signal and background are outlined. These processes are described in detail in [2].

- W production

  The generator EPVEC [7], which uses leading order QCD calculations, was used to estimate the Standard Model expectation for W production. The total W production cross section amounts to 1.1 pb for an electron-proton cms energy $\sqrt{s} = 300$ GeV and 1.3 pb for $\sqrt{s} = 318$ GeV. Final state parton showers are simulated using the PYTHIA framework [8]. An error of 30% is quoted for this cross section calculation. This is due mainly to uncertainties in the photon parton density functions and the scale at which the calculation is performed.

[1] In this paper "electron" refers generically to both electrons and positrons. Where distinction is required the terms e^- and e^+ are used.

- Charged Current (CC) processes : $ep \to \nu X$

  A CC DIS event can mimic the selected topology if a particle in the hadronic final state is misinterpreted as a candidate isolated lepton. The generator DJANGO [9] was used to calculate this contribution. Studies of CC events where a candidate electron, passing loose selection requirements, is found show that events of this kind are described by the expectation within a systematic error of 30% (see section 4).

- Neutral Current (NC) processes : $ep \to eX$

  The scattered electron in a NC DIS event can be identified as an isolated high lepton, but missing transverse momentum can only be produced by fluctuations in the shower or detector response to the final state particles, or by limited geometrical acceptance. The generator DJANGO [9] was used to calculate this contribution. The generator PYTHIA [10] was used to calculate the QCD photoproduction process $\gamma p \to X$. Production of heavy flavours is included in DJANGO and PYTHIA [11]. Studies of NC events with reconstructed missing transverse momentum show that events of this kind are described by the expectation within a systematic error of 30% (see section 4).

- Lepton pair production in two photon ($\gamma\gamma$) interactions

  Inelastic lepton pair production can mimic the selected topology if one lepton escapes detection, and measurement error causes apparent missing momentum. The generator LPAIR [12] was used to calculate this contribution. Studies of events with two identified leptons show that events of this kind are described by the expectation within a systematic error of 75%.

In order to determine acceptances and background contributions for the selected events, the detector response to events produced by the above programs is simulated in detail using a program based on GEANT [13]. The simulated events are then subjected to the same reconstruction and analysis chain as the real data.

3 Experimental Conditions

A detailed description of the H1 detector can be found in [14]. Only those components of particular importance to this analysis are described here.

The inner tracking system consisting of central and forward[2] tracking detectors (drift chambers) are used to measure the charged particle trajectories and to determine the interaction vertex. A magnetic field of 1.15 Tesla allows the measurement of the particle transverse momenta.

Electromagnetic and hadronic final state particles are absorbed in a highly segmented LAr calorimeter [15], which is 5 to 8 interaction lengths deep depending on the polar angle of the particle.

The calorimeter is surrounded by a superconducting coil and an iron yoke instrumented with streamer tubes. Tracks of penetrating charged particles, such as muons, which escape the

[2]The forward direction and the positive z-axis are taken to be that of the proton beam direction.

calorimeter are reconstructed from their hit pattern in the streamer tubes with an efficiency of greater than 90%. The instrumented iron is also used as a backing calorimeter to measure the energy of hadrons that are not stopped in the LAr calorimeter.

In the forward region of the detector two sets of three drift chamber layers (the forward muon system) detect muons and measure their momenta in a toroidal magnetic field. Also in the forward direction, around the beam-pipe, is the plug calorimeter which measures hadronic showers.

The LAr calorimeter is the main trigger for high transverse momentum events. The trigger efficiency is $\approx 98\%$ for events with an electron which has transverse momentum above 10 GeV. For events with high missing transverse momentum, determined from an imbalance in energy measured in the calorimeter, $P_T^{\rm calo}$, the efficiency is 98% when $P_T^{\rm calo} > 25$ GeV and is 50% when $P_T^{\rm calo} = 12$ GeV [16].

4 Lepton identification and Hadronic Reconstruction

An electron candidate is defined by the presence of a compact and isolated electromagnetic cluster of energy in the LAr calorimeter, with the loose requirement of an associated track, having a distance of closest approach to the cluster of less than 12 cm. Electrons found in regions between calorimeter modules containing large amounts of inactive material are excluded [16]. The energy of the electron candidate is measured from the calorimeter cluster.

Muons are identified by requiring tracks in the instrumented iron, the forward muon system, the inner tracking system or any combination. Muon candidates formed from inner tracks alone must be associated with a pattern typical of a minimum ionising particle in the LAr calorimeter. All candidates with an inner track link are required to have transverse momentum above 1 GeV and candidates formed solely by a track in the instrumented iron are rejected for $\theta < 25^\circ$.

A stronger muon identification is required to select the final sample of muon candidates. If the muon candidate is not associated with a forward muon track it must have an inner track link and either a track segment or an energy deposit in the instrumented iron. The momentum of the muon candidate is measured from the curvature of the track in the inner tracking system.

The hadronic final state is measured by combining calorimeter energy deposits with low momentum tracks as described in [16]. The calibration of the final hadronic energy scale is made by comparing the transverse momentum of the precisely measured positron to that of the hadronic final state in a large NC event sample. The ratio of these two measurements is used to correct the hadronic energy measurement as a function of the hadronic polar angle and transverse momentum, typically by less than 10%.

5 Selection of Isolated Electron and Muon Events

Multiple cut requirements must be imposed to remove the background arising from NC, CC, γp and $\gamma\gamma$ interactions, whilst maintaining a good acceptance of Standard Model W decay events. These are listed in tables 1 and 2 and are defined in terms of the quantities described below.

- $P_T^{\rm calo}$, the missing transverse momentum measured in the calorimeter.
- P_T^{miss}, the total missing transverse momentum reconstructed from calorimeters and track detectors.
- P_T^l, the transverse momentum of an identified muon or electron.
- P_T^X, the transverse momentum of the hadronic system, defined as all reconstructed particles apart from identified isolated leptons.
- θ_l, the polar angle of the muon or electron, where $\theta_l = 0^o$ is defined as the direction of the incoming proton beam.
- $\delta_{miss} = 2E_e - \sum E_i(1 - \cos\theta_i)$, where E_i and θ_i denote the energy and polar angle of each detected particle in the event and E_e is the electron beam energy. For an event where only longitudinal momentum in the proton direction is undetected $\delta_{miss} = 0$.
- $\Delta\phi_{l-X}$, the difference in azimuthal angle between the lepton and the vector that balances the vector of the hadronic final state X. NC events typically have low values of $\Delta\phi_{l-X}$.
- V_{ap}/V_p, a measure of the azimuthal balance of the event. It is defined as the ratio of the anti-parallel to parallel components of the measured calorimetric transverse momentum, with respect to the direction of the missing calorimetric transverse momentum [16]. Events with one or more particles, that do not deposit much energy in the calorimeter (μ, ν), generally have low values of V_{ap}/V_p.
- $\zeta_l^2 = 4E^l E_e \cos^2\theta_l/2$, where E^l is the energy of the final state lepton. For NC events, where the scattered electron is misinterpreted as a decay lepton from the W, ζ_l^2 is equal to the four momentum transfer squared Q^2. Since the NC cross section falls steeply with Q^2, these events generally have small values of ζ_l^2. Conversely, leptons from W decay generally have high values of ζ_l^2.
- E_{cone}, the energy contained within a cone of radius 1 in η-ϕ space around the electron, that is not associated to the electron.

The isolation of identified leptons with respect to jets or other tracks in the event, is quantified using:

- their distance D_{jet} to the closest hadronic jet in the pseudorapidity-azimuth plane (η - ϕ), defined by $D_{jet} = \sqrt{(\Delta\eta_{track-jet})^2 + (\Delta\phi_{track-jet})^2}$ (for this purpose jets are reconstructed using an inclusive k_T algorithm [17, 18] with $R < 1$ and $E_T^{min} = 5$ GeV). If there is no jet in the event, D_{jet} is defined with respect to the polar and azimuthal angle of the hadronic final state X.
- their distance D_{track} to the closest track in η - ϕ, defined in an analogous way to D_{jet}, where all tracks with a polar angle greater than 5^o are considered.

The dominant background source in the electron channel arises from NC events which have significant $P_T^{\rm calo}$ due to fluctuations in the measurement of the final state particles. To reduce this background, events with NC topology (azimuthally balanced, with the lepton and hadronic system diametrically opposite in the transverse plane) are rejected. For low values of $P_T^{\rm calo}$, where the NC background is largest, the requirement on ζ_l^2 is tightened. A further requirement that the lepton candidate be isolated from the hadronic final state is imposed to reject CC events. Events which have in addition to the isolated electron one or more isolated muons are not considered in the electron channel, but may contribute in the muon channel.

The dominant backgrounds in the muon channel are due to the inelastic two photon process $ep \rightarrow e\mu^+\mu^- X$ and photoproduction events which contain a muon. The final sample is selected by rejecting azimuthally balanced events and events where more than one muon is observed. Elastic lepton pair production is suppressed by rejecting events which have low track multiplicities and where the muon is found to be opposite in azimuth to the hadron system.

To verify that the backgrounds that contribute to the two channels are well understood, event samples are defined according to less stringent criteria. For the electron channel these criteria are those shown in table 1, but requiring $\zeta^2 > 500$ GeV^2 and the $\frac{V_{ap}}{V_p}$ cut from table 2. For the muon channel these criteria are also those shown in table 1, lowering the P_T^μ threshold to 5 GeV, dropping the P_T^{miss} requirement, but also requiring the $\frac{V_{ap}}{V_p}$ $<$ cut from table 2. Only events with at least one isolated muon satisfying the stronger selection requirements (see section 5) are allowed in the muon sample. The events thus selected in the e^+p data sample are shown in figure 1 for the electron channel and figure 2 for the muon channel. Also included in the figures are the Standard Model expectation and the expectation from W production alone. The electron channel is dominated by NC events and the muon channel is dominated by the two photon process $\gamma\gamma \rightarrow \mu^+\mu^-$. All quantities that are used for the final selection cuts are found to be well described in both shape and normalisation by the Standard Model expectation. Similar agreement between the data and simulation is obtained for the e^-p data sample.

Further studies of individual background processes have also been performed. One example is a subset of the muon sample described above, defined by requiring at least two isolated muons, at least one of which satisfies the stronger selection requirements. This sample is shown in figure 3(a,b). The expectation is dominated by the two photon process $\gamma\gamma \rightarrow \mu^+\mu^-$. The data sample is shown to be well described in both shape and normalisation by the Standard Model expectation.

A second sample was selected from the inclusive sample of CC events[16], with the additional requirement that the electron finder (see section 4) found a candidate electron. This sample is shown in figure 3(c,d). The expectation is dominated by radiative CC events or CC events where a final state particle fakes an electron cluster. The data sample is shown to be well described in both shape and normalisation by the Standard Model expectation.

Following the selection criteria described above, the efficiencies as a function of P_T^X are shown in table 3. These efficiencies were calculated using the EPVEC generator for W production. The overall efficiency to select $W \rightarrow e\nu$ events is 44% and to select $W \rightarrow \mu\nu$ events is 15%. The difference in efficiency between the two channels is due to the cut on $P_T^{\rm calo}$ which acts as a cut on P_T^X because the muon deposits little energy in the calorimeter. There is thus little efficiency in the muon channel for $P_T^X < 12$ GeV. For values of $P_T^X > 12$ GeV the efficiencies of the two channels are comparable at around 44%.

Variable	Requirement
P_T^l	> 10 GeV
θ_l	$5^o < \theta_l < 145^o$
$P_T^{\rm calo}$	> 12 GeV
D_{jet}	> 1.0
P_T^{miss}	> 12 GeV

Table 1: Selection requirements common to both channels.

Variable	Electron	Muon
ζ^2	> 500 GeV^2	-
	> 5000 GeV^2 for $P_T^{\rm calo} < 25$ GeV	-
$\frac{V_{ap}}{V_p}$	< 0.5 (< 0.15 for $P_T^e < 25$ GeV)	< 0.4 (< 0.15 for $P_T^{\rm calo} < 25$ GeV)
D_{track}	> 0.5 for $\theta_e \geq 45^o$	> 0.5
	> 0.5 for $\frac{E_{cone}}{E^l} > 0.05$	
P_T^X	-	> 12 GeV
$\Delta\phi_{e-X}$	$> 20^o$	$> 10^o$ for ≤ 2 central tracks
# isolated μ	0	1
δ_{miss}	> 5 GeV †	-

† *if only one e candidate is detected, which has the same charge as the beam lepton.*

Table 2: Selection requirements specific to each channel.

6 Results

For the e^-p data sample no events are observed in either the electron or muon channels. This compares to the Standard Model expectations of 1.46 $\pm$ 0.30 events in the electron channel and 0.32 $\pm$ 0.09 in the muon channel.

In the e^+p data sample after all selection requirements 10 candidate events are observed in the electron channel compared to 6.08 $\pm$ 1.83 expected from W production and 1.83 $\pm$ 0.45 from background sources. One of the candidate events in the electron channel is observed to contain an e^-. This event was first reported and discussed in [2]. Five of the other candidate events contain an e^+. The charges of the electrons in the remaining events are unmeasured since the electrons are produced at low polar angles and they shower in the material of the tracking detectors. Four of the events in the electron channel have been observed since [4].

For the e^+p data sample in the muon channel 8 candidate events are observed compared to 2.11 $\pm$ 0.63 expected from W production and 0.46 $\pm$ 0.27 from other Standard Model sources. Five of the muon events observed in the e^+p data sample are those first reported and discussed in [2]. Five of the events have positively charged muon, 2 have negative muons and one is not determined.

7 Event kinematics

Distributions of the selected events in lepton polar angle, acoplanarity, transverse mass and P_T^X are shown in figure 4. The figure shows the electron and muon channels combined. Also included is the Standard Model expectation for W production. The events are generally found at low values of lepton polar angle and evenly distributed in acoplanarity in agreement with the expectation. The reduction in the expectation at low and high acoplanarity is due to the selection cuts. The events are distributed in a Jacobian peak consistent with the nominal W mass, as expected from Standard W production. At $P_T^X < 25$ GeV there is good agreement between the expectation and the observed events. At higher values of P_T^X the data lie above the expectation.

The scattered positron is tagged in three of the eighteen events, allowing the lepton-neutrino mass to be reconstructed, under the assumption that there is only one neutrino in the final state and there is no initial state QED radiation. All three events yield masses that are consistent with the W mass, having values of 82^{+19}_{-12}, 71^{+10}_{-11} and 77^{+22}_{-15} GeV. From Standard Model W production it is expected that approximately 25% of events have a scattered positron in the acceptance range of the detector.

The transverse mass and the transverse momentum of the hadronic system of the selected events are compared to W production in figure 5. Events are seen with high P_T^X, atypical of Standard Model W production.

The significance of missing transverse momentum and acoplanarity has been studied with data using a sample of NC events having similar transverse momentum and lepton polar angle to the events selected. The transverse momentum is reconstructed using the calorimetric deposit for comparison with the electron events and using the electron track momentum for comparison with the muon candidates. The deviations from zero in the P_T^{miss} and acoplanarity plane for NC events quantify the experimental smearing. The distribution of this sample is presented in figure 6. This study clearly shows that the observed acoplanarities and missing momenta in the selected events are inconsistent with a measurement error and confirms the existence of a non-detected particle in those events.

Details of the dependence of the event rate for the e^+p data sample as a function of the transverse momentum of the hadronic final state, P_T^X, are given in table 4 and 5 for the electron and muon channels. The combined results for the electron and muon channels are given in table 6. At $P_T^X < 25$ GeV eight events are seen in agreement with the expectation for W production from the Standard Model. At $P_T^X > 25$ GeV ten events are seen six of which are seen at $P_T^X > 40$ GeV where the expectation for Standard Model W production is very low.

8 Summary

A search for events containing an isolated high energy electron or muon, and missing transverse momentum has been performed on an e^+p data sample corresponding to an integrated luminosity of 101.6 pb^{-1} and on an e^-p data sample corresponding to an integrated luminosity of 13.6 pb^{-1}. The selection has been optimised to increase the acceptance of events with a high

energy isolated electron or muon and missing transverse momentum. The analysis also extends to lower values of hadronic transverse momentum P_T^X than have been previously published.

No events are observed in the $e^- p$ data, consistent with the expectations of 1.46 $\pm$ 0.30 and 0.32 $\pm$ 0.09 for the electron and muon channels respectively in this low luminosity data sample. Eighteen events are found in the $e^+ p$ data sample which are kinematically consistent with W production, 10 in the electron channel and 8 in the muon channel. One electron event and 5 of the muon events were first reported and discussed in [2]. The expected rates from the Standard Model are 7.92 $\pm$ 1.88 and 2.56 $\pm$ 0.69 for the electron and muon channels respectively in the $e^+ p$ data sample.

The event rate in both channels is consistent with the expected rate at low values of P_T^X. At $P_T^X > 25$ GeV, however, the 10 observed events exceed the Standard Model prediction of 2.82 $\pm$ 0.73.

Acknowledgements

We are grateful to the HERA machine group whose outstanding efforts have made and continue to make this experiment possible. We thank the engineers and technicians for their work in constructing and now maintaining the H1 detector, our funding agencies for financial support, the DESY technical staff for continual assistance, and the DESY directorate for the hospitality which they extend to the non DESY members of the collaboration.

References

[1] H1 Collab., T. Ahmed et al., DESY preprint 94-248 (1994).

[2] H1 Collab., C. Adloff et al., *Eur. Phys. J.* C 5 (1998) 575.

[3] ZEUS Collab., J. Breitweg et al., *Phys. Lett.* B 471 (2000) 411.

[4] H1 Collab., "W production in ep collisions at HERA", abstract 974, 30th International Conference on High Energy Physics ICHEP2000, Osaka, Japan, July 2000.

[5] N. Malden, "W production in ep collisions", Ph.D. Thesis, Manchester University, November 2000. (http://www-h1.desy.de/publications/theses_list.html)

[6] ZEUS Collab., J. Breitweg et al., "Search for events with isolated high-energy leptons and missing transverse momentum at HERA", abstract #1041 submitted to ICHEP2000 Osaka.

[7] U.Baur, J.A.M. Vermaseren, D.Zeppenfeld, *Nucl. Phys.* B 375 (1992) 3.

[8] C.Diaconu, "Monte Carlo Generators for HERA Physics", Proceedings of the workshop 1998/1999, DESY-PROC-1999-02, p.631.

[9] DJANGO 6.2; G.A. Schuler and H. Spiesberger, Proc. of the Workshop Physics at HERA, W.Buchmüller and G.Ingelman (Editors), (October 1991, DESY-Hamburg) Vol. 3 p.1419.

[10] T. Sjöstrand, Comput. Phys. Commun. **82** (1994) 74.

[11] G. Ingelman, J. Rathsman and G.A. Schuler, Comp. Phys. Comm 101 (1997) 135.

[12] S. Baranov et al., Proc. of the Workshop Physics at HERA, W. Buchmüller and G. Ingelman (Editors), (October 1991, DESY-Hamburg) Vol. 3 p.1478; J.A.M. Vermaseren, *Nucl. Phys.* B 229 (1983) 347.

[13] R. Brun et al., GEANT3 User's Guide, CERN-DD/EE-84-1 (1987).

[14] H1 Collab., I. Abt et al., *Nucl. Instrum. Methods* A 386 (1997) 310 and 348.

[15] H1 Calorimeter Group, B. Andrieu et al., *Nucl. Instrum. Methods* A 336 (1993) 460.

[16] H1 Collab., C. Adloff et al., *Eur. Phys. J.* C 13 (2000) 609.

[17] S.D. Ellis and D.E. Soper, *Phys. Rev.* D 48 (1993) 3160.

[18] S. Catani, Yu.L. Dokshitzer, M.H. Seymour and B.R. Webber, *Nucl. Phys.* B 406 (1993) 187.

	Efficiency	
	e	μ
$P_T^X > 0$ GeV	0.44	0.15
$P_T^X > 12$ GeV	0.40	0.39
$P_T^X > 25$ GeV	0.39	0.49
$P_T^X > 40$ GeV	0.39	0.53

Table 3: Efficiencies of the final selection for W decay in the electron and muon channels as a function of the P_T^X requirement. These efficiencies were calculated with the EPVEC generator.

Electron	Data	SM expectation	W	Other SM processes
$P_T^X > 0$ GeV	10	7.92 ± 1.88	6.08 ± 1.83	1.83 ± 0.45
$P_T^X > 12$ GeV	5	2.57 ± 0.65	2.11 ± 0.63	0.46 ± 0.16
$P_T^X > 25$ GeV	4	1.29 ± 0.33	1.05 ± 0.32	0.24 ± 0.11
$P_T^X > 40$ GeV	2	0.41 ± 0.12	0.40 ± 0.12	0.01 ± 0.01

Table 4: Observed and predicted event rates in the electron channel for all e^+p data.

Muon	Data	SM expectation	W	Other SM processes
$P_T^X > 12$ GeV	8	2.56 ± 0.69	2.11 ± 0.63	0.46 ± 0.27
$P_T^X > 25$ GeV	6	1.54 ± 0.41	1.29 ± 0.39	0.25 ± 0.13
$P_T^X > 40$ GeV	4	0.58 ± 0.16	0.53 ± 0.16	0.05 ± 0.03

Table 5: Observed and predicted event rates in the muon channel for all e^+p data.

Electron and Muon	Data	SM expectation	W	Other SM processes
$P_T^X > 0$ GeV	18	10.48 ± 2.53	8.19 ± 2.46	2.29 ± 0.59
$P_T^X > 12$ GeV	13	5.14 ± 1.31	4.22 ± 1.27	0.92 ± 0.33
$P_T^X > 25$ GeV	10	2.82 ± 0.73	2.34 ± 0.70	0.48 ± 0.18
$P_T^X > 40$ GeV	6	0.99 ± 0.28	0.93 ± 0.28	0.06 ± 0.04

Table 6: Observed and predicted event rates in the electron and muon channels combined for all e^+p data. Only the electron channel contributes for $P_T^X < 12$ GeV.

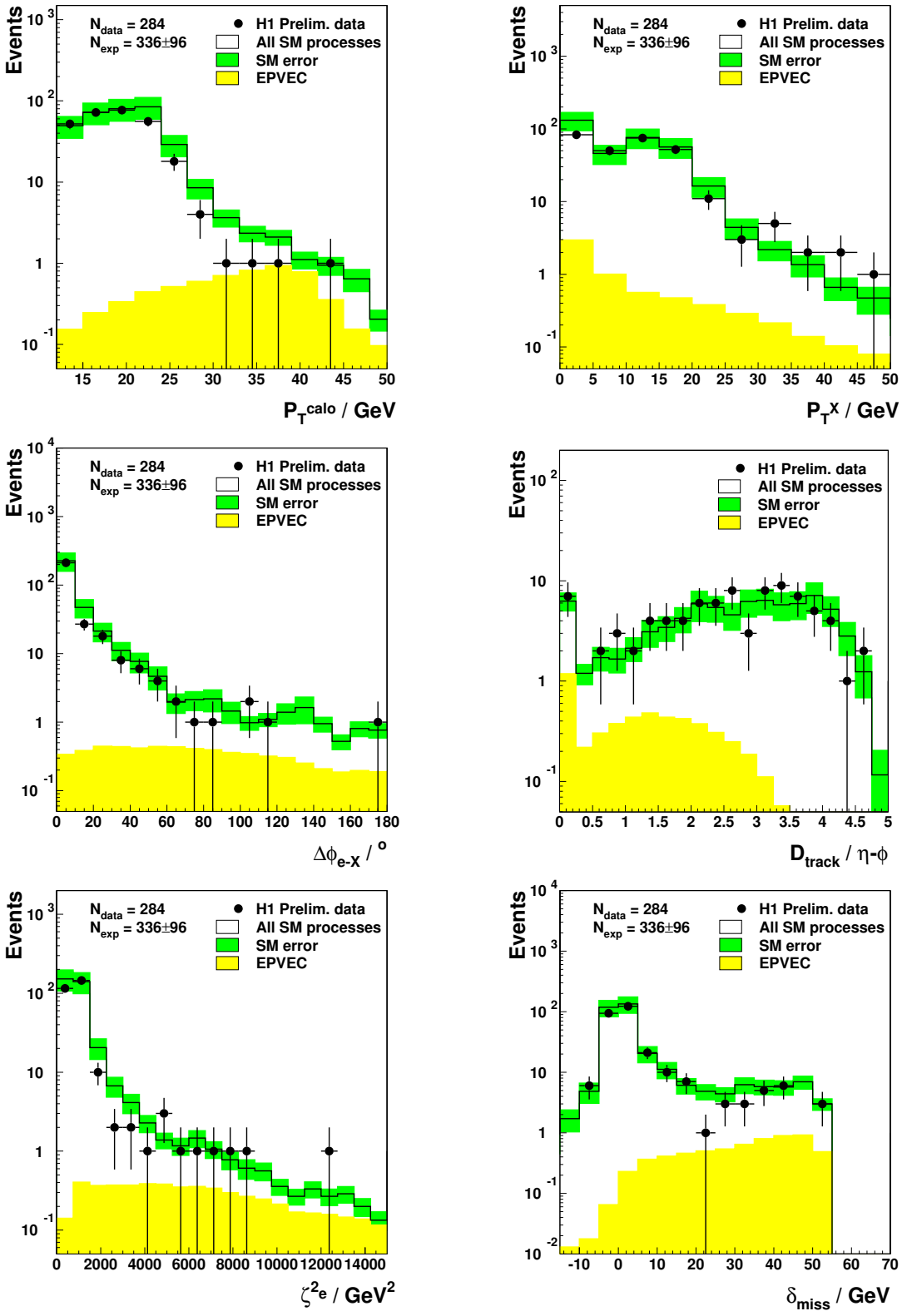

Figure 1: A comparison of the e^+p data selected with the loose requirements in the electron channel compared to the combined Standard Model expectation (open histogram). The total error on the Standard Model expectation is given by the shaded band. The W production component of the Standard Model expectation is given by the shaded histogram.

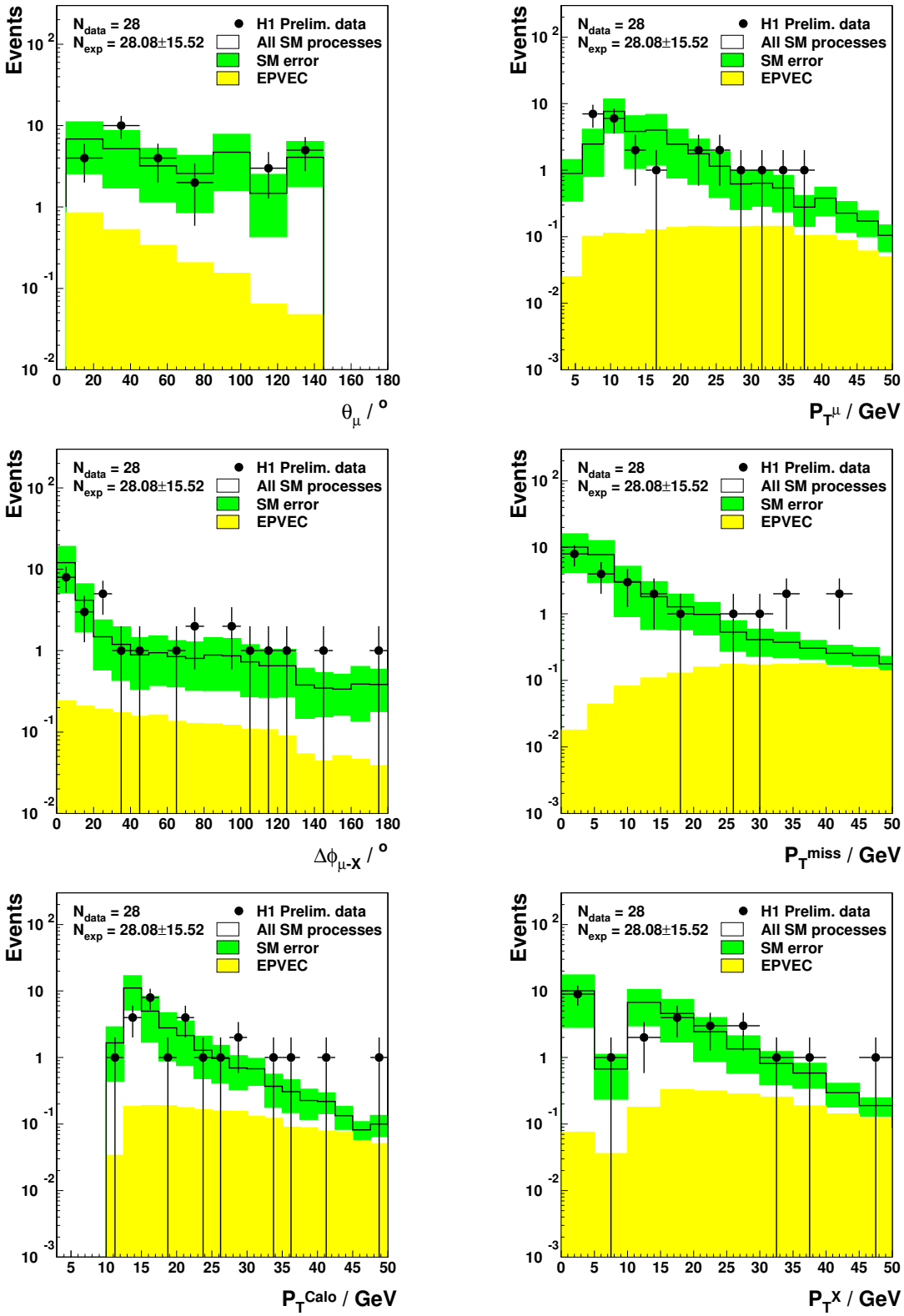

Figure 2: A comparison of the e^+p data selected with the loose requirements in the muon channel compared to the combined Standard Model expectation (open histogram). The total error on the Standard Model expectation is given by the shaded band. The W production component of the Standard Model expectation is given by the shaded histogram.

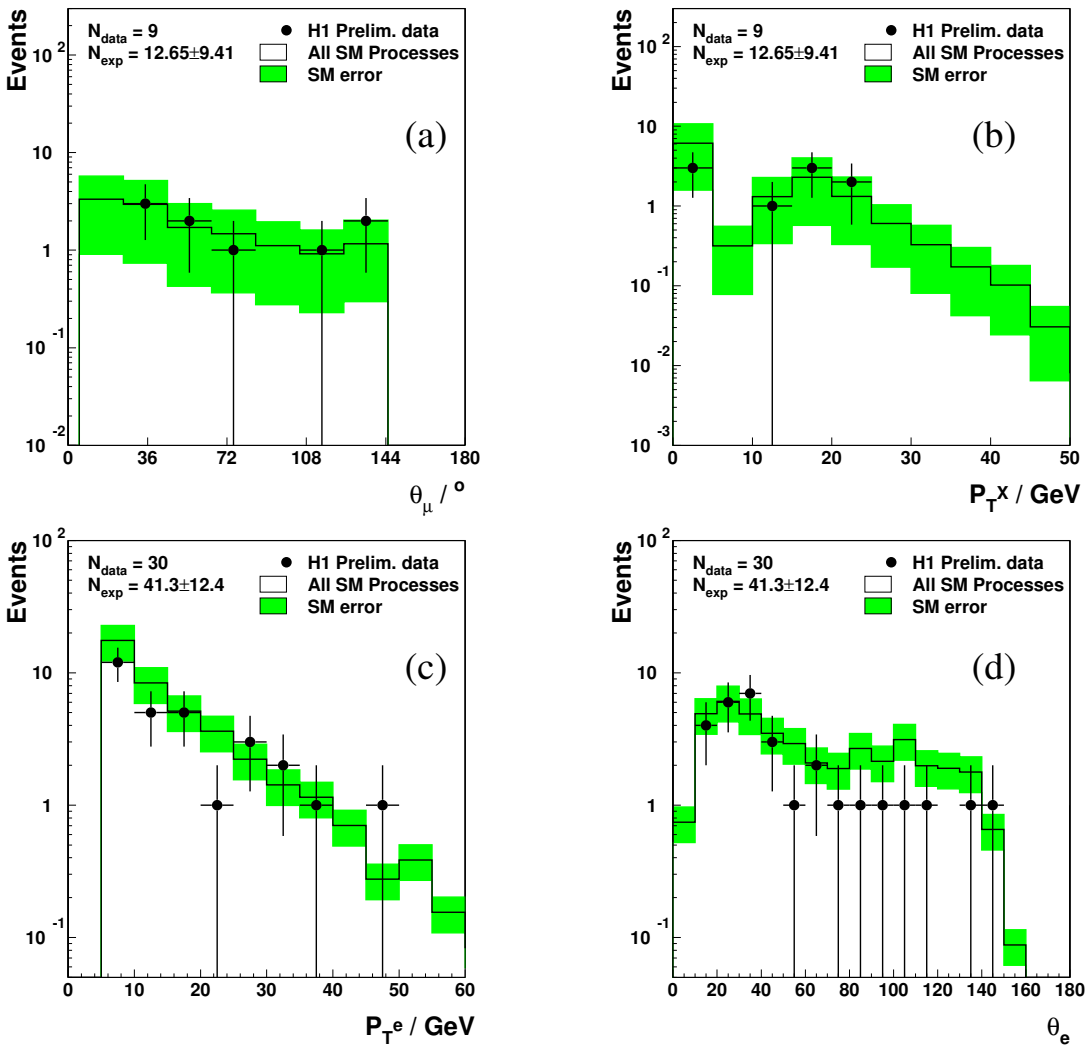

Figure 3: Comparison of a $\gamma\gamma \rightarrow \mu^+\mu^-$ sample ((a) and (b)) and a charged current sample including a candidate electron ((c) and (d)) with the Standard Model expectation. The error on the Standard Model expectation is given by the shaded band.

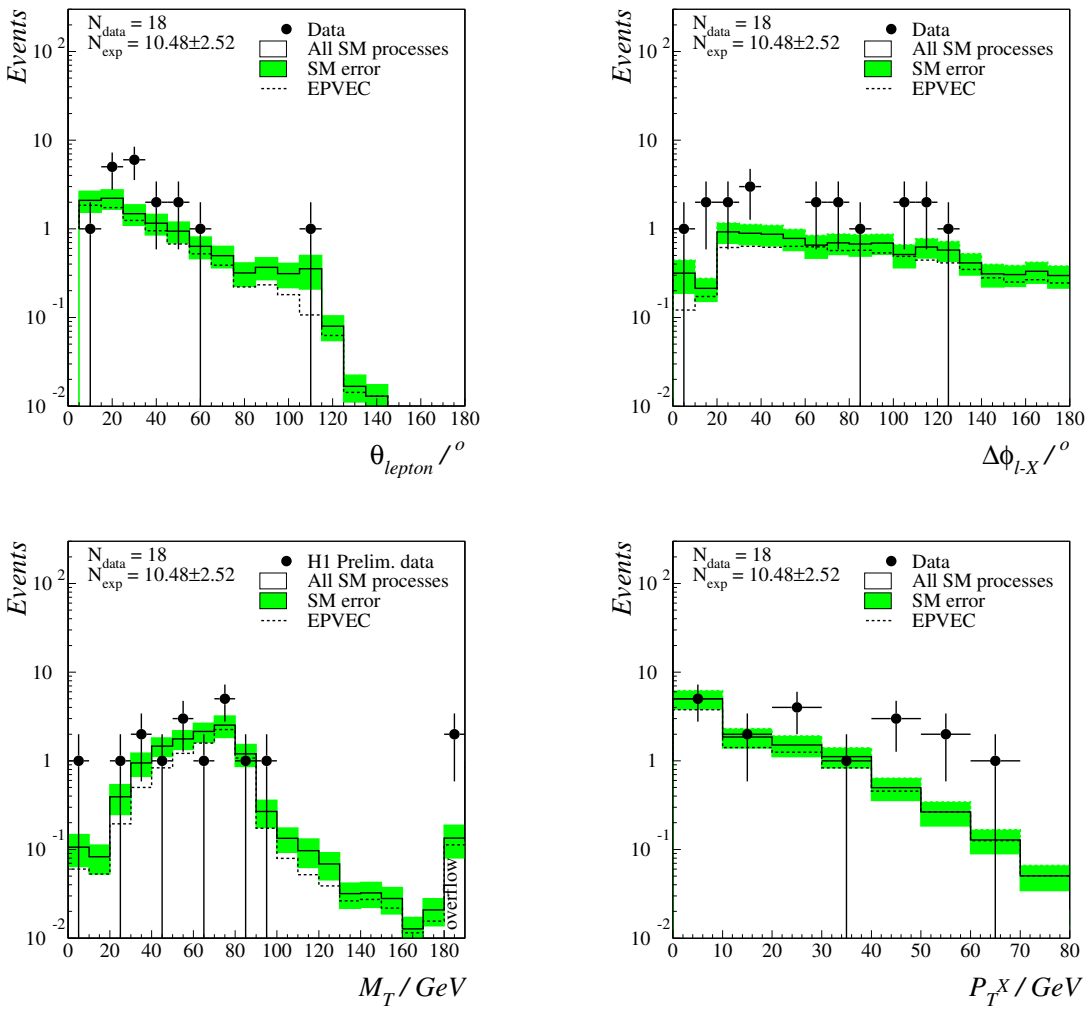

Figure 4: A comparison of the final e^+p data selection in the electron and muon channels combined compared to the combined Standard Model expectation (open histogram). The total error on the Standard Model expectation is given by the shaded band. The W production component of the Standard Model expectation is given by the dashed histogram.

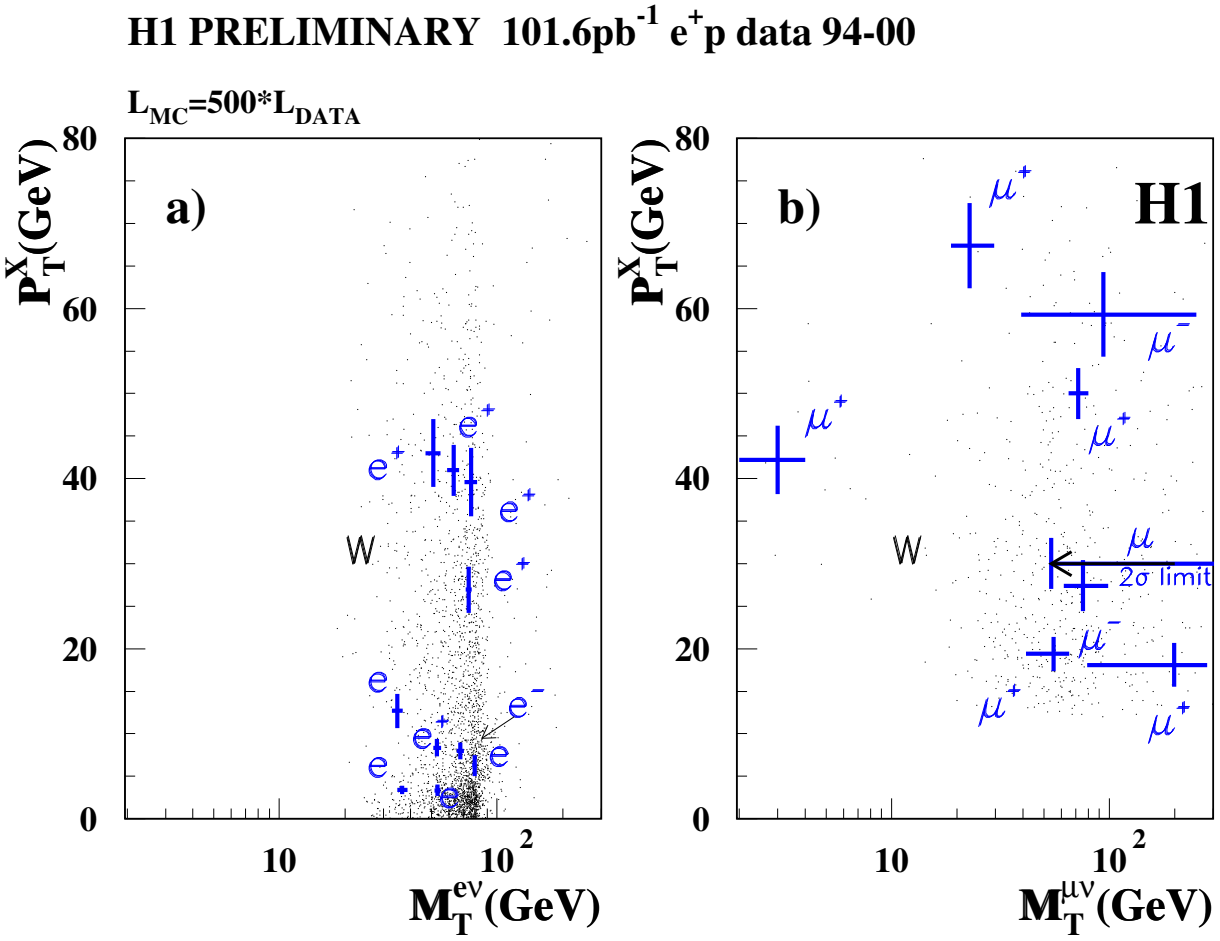

Figure 5: A comparison of the final data sample in each channel, showing the distribution in P_T^X and $M_T^{l\nu}$. The smaller dots represent the distribution of Standard Model W Monte Carlo events with a luminosity 500 times that of the data sample.

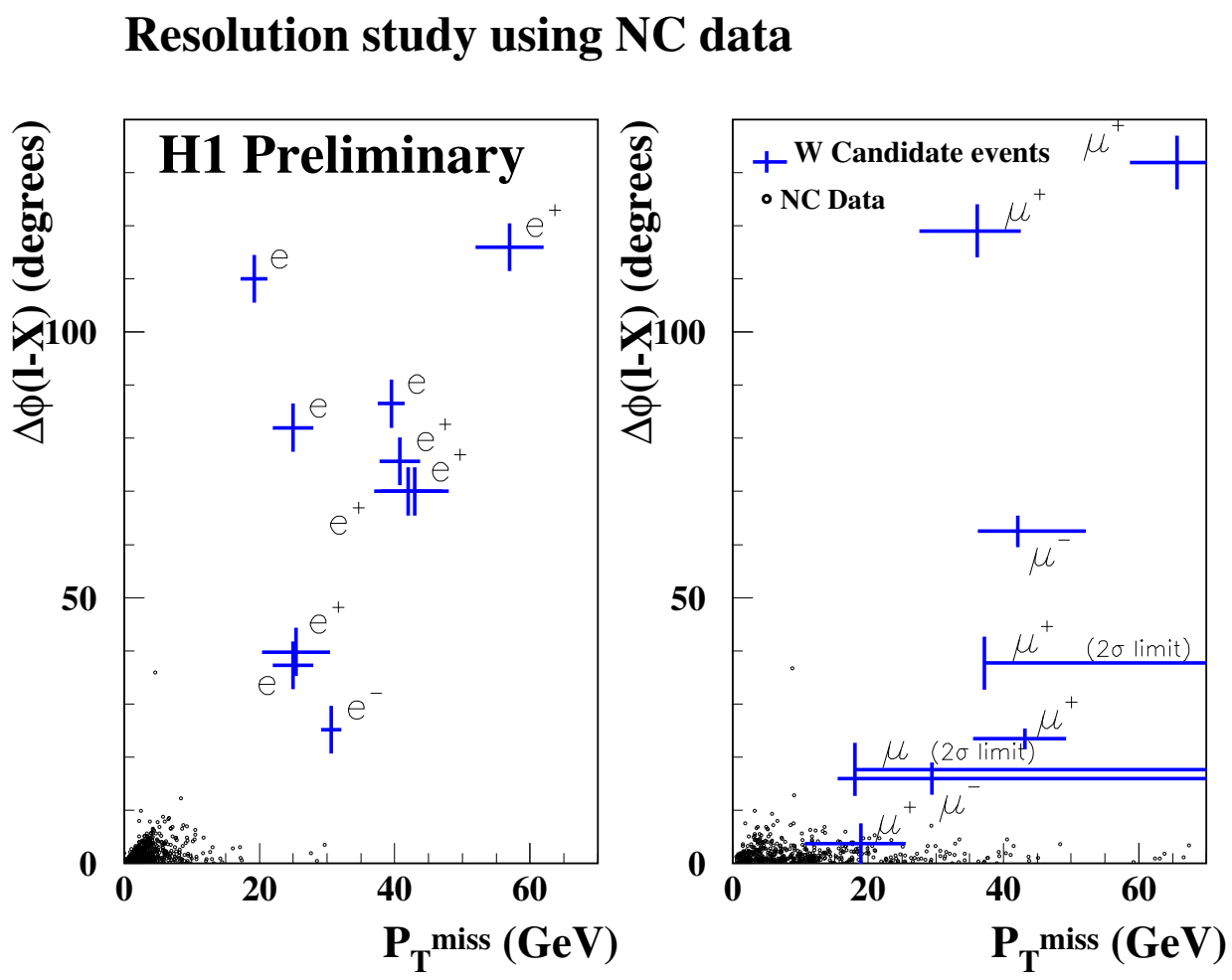

Figure 6: A comparison of the final data sample in each channel, showing the distribution in $\Delta\phi_{l-X}$ and P_T^{miss}. The dots represent the distribution of NC data events.